Power Efficient Magnetization Inversion Using Driven Adiabatic RF Pulses

Michael Carl[1], and Jiang Du[2]
[1]GE Healthcare, San Diego, CA, United States, [2]University of California, San Diego, United States

Introduction: Magnetization inversion is an important tool in MRI to generate contrast and selectively eliminate certain signals in the image, such as fat. While adiabatic pulses have a distinct advantage in that their inversion profile is more robust against B1 and B0 inhomogeneities, some drawbacks include their relatively long duration and high SAR. Unlike non-selective adiabatic pulses, for slice selective adiabatic inversion, the SAR can be reduced by using VERSE corrected pulses [1] with limited peak B1 amplitudes. Here we present modified adiabatic pulses for non-selective inversion, which rotate the magnetization vector along a path parallel to the RF pulse trajectory using driven adiabatic inversion (DAI) pulses. These pulses are capable to achieve similar inversion profiles with shorter durations and SAR than conventional Silver-Hoult (SH) IR pulses [1,2]. Simulations, and phantom experiments were used to compare the inversion efficiency and SAR performance.

Theory: Just like the shortest distance between two points is a straight line, the shortest rotation of a 3D vector between two azimuthal angles is the direct rotation within a single plane. In commonly used adiabatic IR pulses, the magnetization vector (M) nutates around the effective B1 field: $B_{1x}(t)\,i + \Delta\omega(t)/\gamma\,k$, and gets swept from the plus to minus z-axis. During this nutation, M travels in and out of x-z plane of rotation. Our modified pulses are most readily conceptualized using a simple Sin/Cos adiabatic IR pulse with amplitude $B_{1x}(t) = A_0\sin(\xi t)$ and frequency modulation $\Delta\omega(t)/\gamma = A_0\cos(\xi t)$ functions, resulting in a constant rotation sweep $\omega_{sweep} = \xi$ of the B1 vector, and rotation of the magnetization around B1 of $\omega_1 = \gamma A_0$. Fig.1 shows schematic vector diagrams of the effective B1 (black) and M (red). Fig.1A shows the case of a conventional adiabatic IR pulse. The initial offset at t = 0 is exaggerated to emphasize the vector concept. Note how initially the magnetization vector does not get rotated directly downwards along with the sweep rotation of B1 but rather in a direction perpendicular (y-axis). Fig.1B shows the initial configuration for our DAI-modified pulses. The effective B1 field is offset from the z-axis by an angle δ along the y-axis, so that the magnetization vector instantaneously gets rotated towards the x-axis without traveling in and out of the x-z plane. Fig.1C shows the effective B1 and M vector at a later phase during the rotation using DAI pulses. Also shown are the previous vectors from Fig.1B (dotted lines) for reference. Both B1 and M are still at an angle δ, and have undergone the same rotation (rotation angle $\theta = \xi t$) towards the x-axis. To enable the effective B1 field and M to undergone a collinear rotation sweep can be accomplished using the following relation: $\xi = \gamma A_0\tan(\delta)$ (Eq.[1]). The further the initial offset is placed from the z-axis, the faster the radial velocity of the magnetization vector around the B1 axis becomes. For longer pulses the offset angle δ becomes smaller and the DAI pulses approach the corresponding conventional IR pulses.

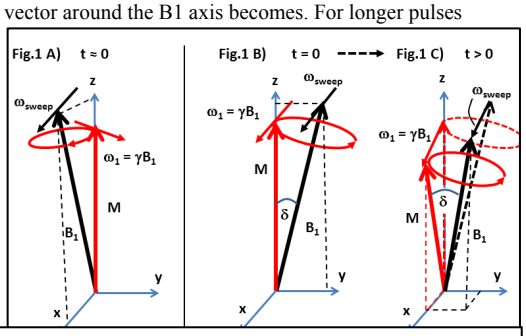

Fig.1: Vector diagrams of the effective B1 and magnetization vector

Simulations: Bloch equations simulations were used to study the effects on the magnetization vector. The three vector components of a conventional Sin/Cos pulse with duration of 2ms, and BW = 1.5kHz are plotted in Fig.2A as a function of time. Fig.2B shows the corresponding trajectory of the magnetization vector. Because M was not able to follow the fast sweep of the B1 field (the adiabatic condition was violated [3]), this IR pulse does not generate a full inversion of the magnetization. Also observe the large oscillations of the y-component of M. When the pulse is stretched to 10ms (not shown) so that the adiabatic condition is better satisfied, results in full magnetization inversion (Fig.2C). Fig.2D shows the modified DAI version of the 2ms pulse shown in Fig.2A. The component along the y-axis is turned on at t = 0 and kept constant during the sweep. Fig.2E shows the corresponding trajectories of M. The magnetization vector follows the trajectory of the x-z component of the effective B1 field (i.e. it follows the most efficient rotation path from plus to minus z) and does generate a full inversion of the magnetization. The same is true when the pulse stretched to 10ms (Fig.2F). The Sin/Cos pulses depicted in Fig.2 are intended to highlight our general concept. To achieve a uniform inversion over a larger BW, SH-IR pulses are more advantageous as a starting point. The same DAI modification can be applied to SH-IR pulses using a generalized form of Eq.[1]. Fig.3 shows 2D plots of the inversion profiles as a function of f_{off} and ΔB1. Shown in A) and B) are results for the conventional, and DAI-modified Sin/Cos pulses (shown in Figs.2 A and D). Also shown in part C) and D) are the results for a 7ms DAI-modified SH-IR pulse with μ = 4 and BW of 1.25kHz and conventional 8.6ms SH-IR pulse with μ = 5 and BW of 1.25kHz. As can be seen from Fig.3, the conventional and DAI-modified SH-IR pulses exhibit much sharper spectral transition regions than the short Sin/Cos pulses. As already observed in Fig.2B, the conventional Sin/Cos pulse does not result in full magnetization inversion even at $f_{off} = \Delta B1 = 0$, while the DAI-modified version does (see Fig.3B).

Experiments: The experimental setup consisted of a large cylindrical water phantom, as well as smaller spherical fat and short T2 phantoms (1ms and 0.3ms). Axial 2DUTE images are shown in Fig.4 using TE = 12μs (A), and TE = 1000μs (B). The image Fig.4C was obtained at the null-point of a 3ms DAI SH-IR pulse and TE = 12μs. Fig.5 shows the spectral responses of several IR pulses (conventional and DAI) with various durations. Shown as blue circles are the results for a conventional 8.6ms SH-IR pulse (normalized SAR = 1). The results of a DAI-modified 7ms SH-IR (SAR = 0.76) and a DAI-modified 3ms SH-IR pulse (SAR = 0.45) are shown as red squares and black triangles, respectively. All pulses resulted in full inversion, however some of the flat inversion profile is sacrificed for the 3ms pulse, as expected.

Conclusion: We developed adiabatic pulses for non-selective inversion, which drive the magnetization vector along a path parallel to the effective B1 trajectory using driven adiabatic inversion (DAI) pulses. These pulses may play a particularly important role in IR prepared 3DUTE imaging [4], where the minimum TR (and hence scan-time) is limited by the SAR imparted by the adiabatic inversion pulses. Simulations, and phantom test were performed and show that the inversion efficiency compares well to conventional Silver-Hoult IR pulses, while significantly reducing the imparted SAR.

References: [1] Conolly et al, JMR 78,440-458 (1988) [2] Silver et al, JMR 59, 347-351 (1984)
[3] M. A. Bernstein et al, *Handbook of MRI Pulse Sequences* (2004) [4] Du et al, MRI 29 (2011) 470–482

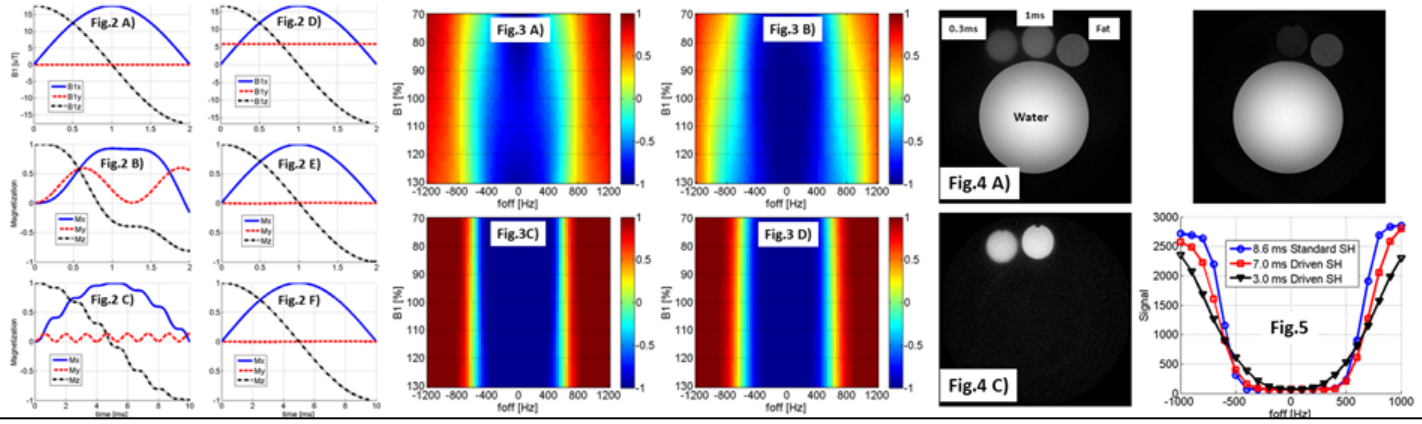

Fig.2: Evolution of effective B1 and magnetization vectors. Fig.3: Inversion profiles as as a function of f_{off} and ΔB1. Fig.4: 2DUTE images of the phantom Fig.5. Spectral responses from IR pulses